
Non-conservation of linear momentum in widely used hierarchical methods in gravitational gas dynamics

A Preprint

✉ Marat Sh. Potashov^{*1,2} and ✉ Andrey V. Yudin²

¹Keldysh Institute of Applied Mathematics, Miusskaya sq., 4, Moscow, Russia

²National Research Center “Kurchatov Institute”, Kurchatov sq., 1, Moscow, Russia

2024 year

Abstract

The paper considers the implementation of the fast multipole method (FMM) in the PHANTOM code for the calculation of forces in a self-gravitating system. The gravitational interaction forces are divided into short-range and long-range interactions depending on the value of the tree opening parameter of the hierarchical kd-tree. It is demonstrated that Newton’s third law holds for any pair of cells of the kd-tree engaged in mutual interaction. However, for the entire system a linear momentum is not conserved. As a result, there is an unphysical force that causes the center of mass to migrate. For example, for a pair of neutron stars, the displacement of the system’s center of mass is found to be comparable to the radii of the objects at times of a few tens of Keplerian revolutions. This displacement cannot be reduced by increasing the number of particles for values of the tree opening parameter greater than 0.2. For smaller values, the time required for the calculation is significantly longer.

Keywords tree code · fast multipole method · FMM · momentum conservation · N-body · smoothed particle hydrodynamics · SPH · PHANTOM

1. Introduction

The number of computations required to accurately calculate the forces in a self-gravitating system, acting between a set of N particles, grows with the increase of the number of particles as a function of $\mathcal{O}(N^2)$. This makes calculations involving tens of thousands of particles practically impossible. Several alternatives have been proposed to solve the problem of quadratic growth in computational costs for self-gravity. These include the tree-code method [1], the fast multipole method (FMM) [2–5], and hybrid methods combining elements of particle mesh approaches [6] and the FMM [7; 8].

The computational complexity of Barnes-Hut method [1] is $\mathcal{O}(N \log N)$. Many FMM implementations, including those presented in [9–11], yield a linear complexity $\mathcal{O}(N)$. Moreover, there are even such realizations of FMM [12] whose computational cost achieves $\mathcal{O}(N^{0.87})$ operations with comparable errors.

The aforementioned methods are based on the concept of collecting particles into hierarchically structured groups (cells) forming a tree. This enables to carry out the costly computational calculations, wherein the forces of gravitational attraction are taken into account at the level of the cell as a whole, rather than on an individual particle basis. Different codes use various kinds of trees. An octree, which is generated by dividing each cell into eight subcells, is considered within the tree-code [1; 9; 10] and *Octo-Tiger* [13]. The binary kd-tree [14] is employed by the code PKDGRAV3 [15], which is used in cosmological simulations. Additionally, it is utilised in codes based on the method of the smoothed particle hydrodynamics (SPH) such as [11] and PHANTOM [16; 17].

*marat.potashov@gmail.com

This article discusses the implementation of the FMM in the 3D SPH magnetohydrodynamic code PHANTOM. In computational astrophysics, the FMM is one of the most prevalent, while the PHANTOM code is successfully used in various fields of astrophysics [18–23]. The current implementation of FMM in PHANTOM in Cartesian coordinates demonstrates the complexity $\mathcal{O}(N \log N)$. However, as will be showed, this implementation does not conserve the total linear momentum of the system. This article complements and revises an earlier paper [24].

The article is structured in the following way. In the section 2 we briefly describe the PHANTOM code and its implementation of the method for calculating the self-gravity forces. In the section 3 we prove the fulfilment of Newton’s third law for any pair of kd-tree cells in the case of mutual interaction. In section 4 it is shown that the way of describing the interaction for the whole system in the PHANTOM code does not satisfy the third law, resulting in the generation of a non-physical force. In the section 5 we demonstrate how the center of mass of the system migrates due to this force. In the section 6 the non-conservation of linear momentum for the whole system in the PHANTOM calculations is illustrated by the example of a single neutron star (NS). It is also shown which factors affect this non-conservation. In the final section 7 we conclude that there is a need to change the code PHANTOM, for example, based on the works [9; 10].

2. Description of the self-gravity forces in PHANTOM

The PHANTOM code uses SPH — it’s a Lagrangian meshless method. Particles in the SPH method are volumetric elements of the medium with unspecified shape, which are assigned to physical characteristics: coordinates, speed, mass, density, characteristic size, temperature, pressure and so on. A restriction is introduced in PHANTOM: all particles have the same mass. Discrete representation of the medium as a set of smoothed particles implies replacement of continuous characteristics $f(r)$ by piecewise-constant quantities f_i . For each particle i , these values are calculated by summing the values f_j of neighbouring particles j , where each summand is weighted by a special function called the smoothing kernel. The approximation of spatial derivatives in the right-hand sides of the conservation laws equations in SPH is achieved by transferring the particle coordinate derivatives to the derivative of the smoothing kernels. Using the solutions of the equations of motion, continuity, and energy, in the form of the SPH approximation, one can describe how the density, temperature, and pressure of matter described by SPH particles will change [16].

Henceforth, we’ll use a system of units, in which the unit of time is

$$u_{\text{time}} = \sqrt{\frac{u_{\text{dist}}^3}{G u_{\text{mass}}}}, \quad (1)$$

where u_{dist} and u_{mass} are the units of distance and mass respectively and G is the Newtonian constant of gravitation.

To obtain the acceleration of SPH-particles \mathbf{a}_{grav} caused by the self-gravitational forces, we need to find the gravitational potential Φ that satisfies the Poisson equation, which is written in our system of units as

$$\nabla^2 \Phi = 4\pi \rho(\mathbf{r}), \quad (2)$$

where ρ is the density of the matter. Then the corresponding acceleration will be $\mathbf{a}_{\text{grav}} = -\nabla \Phi$.

The elliptic type equation (2) implies an instant action. Consequently, the solution must be global for the whole system. One chosen particle is affected by all other particles, both near and far. Such a solution is found in PHANTOM by representing of the total acceleration of the SPH-particle as the sum of the accelerations resulting from the short-range and long-range interactions:

$$\mathbf{a}_{\text{grav}} = \mathbf{a}_{\text{short}} + \mathbf{a}_{\text{long}}. \quad (3)$$

The splitting (3) is dictated by the considerations of computational optimization. The way of calculating the two types of acceleration is different.

To determine which interactions are considered to be short-range and which are to be long-range, the following procedure is performed. All SPH-particles of the system are hierarchically grouped into cells of the kd-tree. The algorithm recursively cuts the cells through their centers of mass and forms new subcells by splitting the longest axis into two parts in order to leave the cells with a more compact shape. This allows to reduce errors when cutting off their multipole expansion [11]. The procedure stops for cells containing not more than 10 SPH-particles. Such cells are called leaf cells, and those higher up in the hierarchy are called super-cells.

Let us consider two arbitrary not necessarily leaf cells α and β , the distance between their centers of mass is denoted by r . The particles of the first cell interact with the second cell in a short-range manner when one of the two criteria is satisfied. The first of them is the tree opening criterion:

$$\theta^2 < \left(\frac{s_\beta}{r}\right)^2, \quad (4)$$

where $0 \leq \theta \leq 1$ is the tree opening parameter. Here, s is the size of the cell, which is equal to the minimum radius of the sphere centered on the center of mass of the cell, and containing all its SPH-particles. Note also that for $\theta = 0$, the tree opening criterion (4) is always satisfied and $\mathbf{a}_{\text{grav}} = \mathbf{a}_{\text{short}}$. In this case, all accelerations in the system are calculated by direct summation.

The second criterion describes the possibility of intersecting smoothing spheres for SPH-particles of different cells:

$$r^2 < [s_\alpha + s_\beta + \max(R_{\text{kern}}h_{\text{max}}^\alpha, R_{\text{kern}}h_{\text{max}}^\beta)]^2. \quad (5)$$

Here h_{max} is the maximum smoothing length among all the particles in the cell, and R_{kern} is the dimensionless cut-off radius of the smoothing kernel $W(h)$. A sphere of radius $R_{\text{kern}}h$ is a compact support of the kernel $W(h)$. If distances from the center of the particle are larger than $R_{\text{kern}}h$, all physical quantities described by SPH-particle are assumed to be zero.

The near acceleration $\mathbf{a}_{\text{short}}$ is calculated by direct summation over neighbouring particles (see [17; 25]). Gravitational potential for SPH-particles, smoothed by the kernel $\phi(\epsilon)$ for points with $r > R_{\text{kern}}\epsilon$, behaves like $1/r$. A function has no compact support. If one uses only near acceleration to calculate the gravitational force for the whole system, then all the conservation properties are fulfilled, namely conservation of linear momentum, angular momentum and energy [17; 25].

The following procedure is used to calculate the long-range acceleration component \mathbf{a}_{long} in PHANTOM. The components of the gravitational acceleration of a particular cell α caused by the gravitational attraction of another cell β are obtained by multipole expansion of the acceleration in powers of $1/r$:

$$a_{\beta \rightarrow \alpha, i}(\mathbf{r}) = -\frac{M_\beta}{r^2} \hat{r}_i + \frac{1}{r^4} \left(\hat{r}_k Q_{\beta, ik} - \frac{5}{2} \hat{r}_i \hat{r}_j \hat{r}_k Q_{\beta, jk} \right). \quad (6)$$

Here \mathbf{r} is a vector connecting the centers of mass of cells α and β , r is its length, and \hat{r}_i are the components of the corresponding unit vector, M_β is the total mass of the cell β ,

$$Q_{\beta, ij} = \sum_{\mathbf{y} \in \beta} m_p [3y_i y_j - y^2 \delta_{ij}] \quad (7)$$

is the quadrupole moment of the cell β , \mathbf{y} is the radius vector starting at the center of mass of the cell to some particle inside the cell, and m_p is the mass of the particle, which in PHANTOM is assumed to be the same for all particles.

Consider some SPH-particle inside the cell α with the radius vector \mathbf{x} starting at the center of mass of the cell α . The components of the gravitational acceleration of this SPH-particle caused by interaction with the β cell are obtained by Taylor expansion of $a_{\alpha \rightarrow \beta, i}$ up to the second order for small displacements \mathbf{x} from \mathbf{r} :

$$a_{\beta \rightarrow \alpha, i}(\mathbf{r}, \mathbf{x}) = a_{\beta \rightarrow \alpha, i}(\mathbf{r}) + x_j \frac{\partial a_{\beta \rightarrow \alpha, i}(\mathbf{r})}{\partial r_j} + \frac{1}{2} x_j x_k \frac{\partial^2 a_{\beta \rightarrow \alpha, i}(\mathbf{r})}{\partial r_j \partial r_k}. \quad (8)$$

This approach is called the fast multipole method [2]. In PHANTOM it is implemented in Cartesian coordinates. Using the notation of the paper [12], one can state that the steps required to determine the acceleration \mathbf{a}_{long} in PHANTOM are: step P2M (particle to multipole), consisting in calculation of Q_{ij} in accordance to equation (7), step M2L (multipole to local expansion), involving the use of equation (6), and finally step L2P (local expansion to particle) that includes the utilization of equation (8).

In the next section we prove the fulfillment of Newton's third law for any pair of cells, all particle accelerations in which are described by the formula (8).

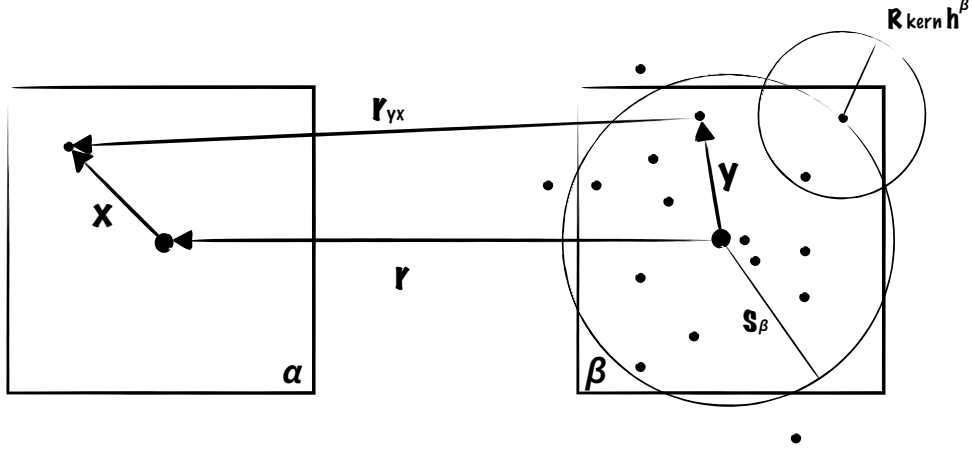


Figure 1. Gravitational interaction of SPH-particles of the α cell with SPH-particles of the β kd-tree cell. Details in the text.

3. Symmetric interaction of a pair of kd-tree cells

Consider a pair of kd-tree cells α and β (see Figure 1), which are sufficiently distant from each other so that their parameters do not satisfy the criteria (4), (5). In this case, we will refer to such cells as well-separated. The minimum radius of the sphere located at the center of mass of the cell β containing all its SPH-particles, designated as s_β , and the maximum smoothing length among all particles of the cell β , designated as h_{\max}^β , are shown in Fig. 1. The cells α and β are not necessarily leaf cells. We denote the total cell masses as M_α and M_β correspondingly.

Let the radius vectors of SPH-particles inside the cells α and β originating from their centers of mass be denoted by \mathbf{x} and \mathbf{y} , respectively. Let us also introduce a vector \mathbf{r} between the centers of mass of the cells α and β and its length $r = |\mathbf{r}|$. Then the distance between two arbitrary particles of different cells is

$$r_{yx} = |\mathbf{r} + \mathbf{x} - \mathbf{y}|. \quad (9)$$

In order to determine the potential created by all particles of the cell β at the point \mathbf{x} of the cell α , we need to find the solution of the Poisson equation (2) in the outer region of the β zone. We will assume the potential to be equal to zero at infinity. The solution of such a problem (see, e.g., [26]) is defined by the expression

$$\Phi_{\beta \rightarrow \alpha}(\mathbf{x}) = \int_{\beta} \rho(\mathbf{y}) G(\mathbf{r} + \mathbf{x}, \mathbf{y}) d^3 y, \quad (10)$$

where $G(\mathbf{r} + \mathbf{x}, \mathbf{y})$ is the Green's function of the Laplace operator, which is symmetric with respect to permutation

$$(\alpha, \mathbf{x}, \mathbf{r}) \Leftrightarrow (\beta, \mathbf{y}, -\mathbf{r}). \quad (11)$$

It can be shown [25] that for a variable smoothing length $h(\mathbf{y})$ which depends on the density and is a function of the spatial variable, the expression (10) in the SPH approximation converts to

$$\Phi_{\beta \rightarrow \alpha}(\mathbf{r}, \mathbf{x}) = \sum_{\mathbf{y} \in \beta} m_p G(\mathbf{r} + \mathbf{x}, \mathbf{y}), \quad (12)$$

where

$$G(\mathbf{r} + \mathbf{x}, \mathbf{y}) = -\frac{\phi(r_{yx}, h(\mathbf{x})) + \phi(r_{yx}, h(\mathbf{y}))}{2}. \quad (13)$$

Here the smoothing kernel ϕ for the potential is determined from the solution of the Poisson equation

$$W(z, h) = \frac{1}{4\pi z^2} \frac{\partial}{\partial z} \left(z^2 \frac{\partial \phi}{\partial z} \right),$$

where $z \equiv r_{yx}$. For the standard smoothing kernels $W(z, h)$ and from (13) for

$$r_{yx} > R_{\text{kern}} h \quad (14)$$

one can obtain (see [17; 25])

$$G(\mathbf{r} + \mathbf{x}, \mathbf{y}) = -\frac{1}{r_{yx}}. \quad (15)$$

The i -component of the acceleration of a SPH-particle at the point \mathbf{x} caused by its attraction by the entire cell β is

$$a_{\beta \rightarrow \alpha, i}(\mathbf{r}, \mathbf{x}) = -\frac{\partial \Phi_{\beta \rightarrow \alpha}(\mathbf{r}, \mathbf{x})}{\partial x_i} = -\sum_{\mathbf{y} \in \beta} m_p \frac{\partial G(\mathbf{r} + \mathbf{x}, \mathbf{y})}{\partial x_i}. \quad (16)$$

The components of the total force acting on the cell α from the side of cell β are obtained by summing (16) for all SPH-particles of the cell α :

$$F_{\beta \rightarrow \alpha, i}(\mathbf{r}) = -\sum_{\mathbf{x} \in \alpha, \mathbf{y} \in \beta} m_p^2 \frac{\partial G(\mathbf{r} + \mathbf{x}, \mathbf{y})}{\partial x_i}. \quad (17)$$

Due to the symmetry of the Green's function with respect to permutation (11), the resulting expression is symmetric: $F_{\beta \rightarrow \alpha, i} = F_{\alpha \rightarrow \beta, i}$. Since inequality (14) is fulfilled for well-separated cells, the Green's function has a simple form (15). Therefore, the gravitational interaction force (17) between such cells does not depend on the parameters of the SPH method. This approach is consistent with the N-body formalism.

By summing (16) over all cells β , we get the total acceleration of the SPH-particle at the point \mathbf{x} . Even taking into account the symmetry of the Green's function with respect to permutation (11), it is clear that to calculate the behavior of all N SPH-particles in the system it is necessary $\propto N^2$ times to take the derivative of it at large N . As was described in section (1), several alternative methods have been proposed to solve the problem of quadratic computational complexity. Some of them demonstrate the complexity of $\mathcal{O}(N^{0.87})$ for comparable errors. This speed gain is largely due to the recursive way of traversing the tree and finding mutually-symmetrically interacting cells [9]. However, all these methods share a common property: they replace the ‘‘particle–particle’’ interactions with other types of interactions, such as ‘‘particle–cell’’ and ‘‘cell–cell’’ interactions. To implement this, a multipole extension is used.

The Taylor expansion of Green's function (15) around \mathbf{r} to order p reads

$$G(\mathbf{r} + \mathbf{x}, \mathbf{y}) = \sum_{|n|=0}^p \sum_{|m|=0}^{p-|n|} \frac{x^n y^m}{n! m!} \left. \frac{\partial^{|n|+|m|} G(\mathbf{r} + \mathbf{x}, \mathbf{y})}{\partial x^n \partial y^m} \right|_{\substack{\mathbf{x}=\mathbf{0} \\ \mathbf{y}=\mathbf{0}}} + R_p(\mathbf{r} + \mathbf{x}, \mathbf{y}). \quad (18)$$

Here we use multi-indices notation (see, e.g., [12; 27]), which is more convenient than tensor notation in this case. The first sum corresponds to a triple summation for each component of \mathbf{x} , where the sum of the indices $|n| = n_{x_1} + n_{x_2} + n_{x_3} \leq p$. The second sum corresponds to a triple summation for component of \mathbf{y} , where the sum of the indices $|m| = n_{y_1} + n_{y_2} + n_{y_3} \leq p - |n|$. The residual term of the Taylor formula is R_p . Let us define the following notations:

$$\begin{aligned} x^n &\equiv x_1^{n_{x_1}} x_2^{n_{x_2}} x_3^{n_{x_3}}, & y^m &\equiv y_1^{n_{y_1}} y_2^{n_{y_2}} y_3^{n_{y_3}}, \\ n! &\equiv n_{x_1}! n_{x_2}! n_{x_3}!, & m! &\equiv n_{y_1}! n_{y_2}! n_{y_3}!, \\ \partial x^n &\equiv \partial x_1^{n_{x_1}} \partial x_2^{n_{x_2}} \partial x_3^{n_{x_3}}, & \partial y^m &\equiv \partial y_1^{n_{y_1}} \partial y_2^{n_{y_2}} \partial y_3^{n_{y_3}}. \end{aligned} \quad (19)$$

The gradient of the Green's function at the point $\mathbf{x} = \mathbf{y} = 0$ depends only on \mathbf{r}

$$\left. \frac{\partial^{|n|+|m|} G(\mathbf{r} + \mathbf{x}, \mathbf{y})}{\partial x^n \partial y^m} \right|_{\substack{\mathbf{x}=\mathbf{0} \\ \mathbf{y}=\mathbf{0}}} = (-1)^{|m|} \partial^{n+m} G(\mathbf{r}, 0), \quad (20)$$

where we use the following shortened form:

$$\partial^{n+m} f \equiv \frac{\partial^{|n|+|m|} f}{\partial r^{n+m}}, \quad (21)$$

$$\partial r^{n+m} \equiv \partial r_1^{n_{x_1} + n_{y_1}} \partial r_2^{n_{x_2} + n_{y_2}} \partial r_3^{n_{x_3} + n_{y_3}}. \quad (22)$$

Substituting (18) into (12) and taking into account (20), after regrouping the terms we have

$$\Phi_{\beta \rightarrow \alpha}(\mathbf{r}, \mathbf{x}) = \sum_{|n|=0}^p \frac{x^n}{n!} \sum_{|m|=0}^{p-|n|} M_m \partial^{n+m} G(\mathbf{r}, 0) + \sum_{\mathbf{y} \in \beta} m_p R_p(\mathbf{r} + \mathbf{x}, \mathbf{y}), \quad (23)$$

where

$$M_m = \sum_{\mathbf{y} \in \beta} m_p \frac{(-1)^{|m|}}{m!} y^m \quad (24)$$

are multipole moments. Setting $p = 3$ in the formula (23) and neglecting the octopoles $M_3 = 0$, we obtain the expressions from [9; 10].

Differentiating the gravitational potential (23) with respect to x_i and taking into account (16), we get

$$a_{\beta \rightarrow \alpha, i}(\mathbf{r}, \mathbf{x}) = \sum_{|n|=0}^{p-1} \frac{x^n}{n!} \partial^n a_{\beta \rightarrow \alpha, i}(\mathbf{r}) + \tilde{R}_p(\mathbf{r}, \mathbf{x}), \quad (25)$$

where

$$a_{\beta \rightarrow \alpha, i}(\mathbf{r}) = - \sum_{|m|=0}^{p-1-|n|} M_m \partial^{m+1} G(\mathbf{r}, 0) \quad (26)$$

and $\tilde{R}_p(\mathbf{r}, \mathbf{x})$ is a residual term. For $p = 3$, the series (25) is similar to the acceleration expression in PHANTOM (8). However, there are differences. In the equation (8) the highest degree of $1/r$ in the third term of the corresponding Hessian matrix is equal to 6. In the equation (25) this degree derived from $\partial^3 G(\mathbf{r}, 0)$ is equal to 4.

To obtain the desired degrees, we carry out the following procedure: we write out the series (25) for $p = 5$, discarding all terms with $n = 3, n = 4, m = 3, m = 4$, excluding octopoles and higher orders of x and y . The final series differs from the series (25) at $p = 3$ in that it has three additional terms with pairs of indices

$$(n, m) = (1, 2); (2, 1); (2, 2), \quad (27)$$

whose sum is less than the value of the residual term $\tilde{R}_3(\mathbf{r}, \mathbf{x})$, remaining within this error. The final expressions are

$$a_{\beta \rightarrow \alpha, i}(\mathbf{r}, \mathbf{x}) \approx \sum_{|n|=0}^2 \frac{x^n}{n!} \partial^n a_{\beta \rightarrow \alpha, i}(\mathbf{r}) \quad (28)$$

and

$$a_{\beta \rightarrow \alpha, i}(\mathbf{r}) = \sum_{|m|=0}^2 M_m \partial^{m+1} G(\mathbf{r}, 0). \quad (29)$$

They coincide with expressions (8) and (6) respectively.

One can give another description of the difference between the approaches (24)–(26) and (6)–(8). We will call all particles of the cell α as sinks and particles of the cell β as sources. Then the approach (24)–(26) involves a Taylor expansion over small displacements from \mathbf{r} of both source and sink so that their combined order is not greater than $(p - 1)$. And the approach (6)–(8) is a successive expansion first by small displacements from \mathbf{r} of the source to order $(p - 1)$ and only then by small displacements of the receiver to order $(p - 1)$.

Now let's go back to the expression (18). It is symmetric with respect to permutation (11) at every order of precision. However, the symmetry of this expression will not be changed if we carry out the procedure described above by adding to the series (18) at $p = 3$ the pairs (27), which are symmetric by indices as well. Substitution of the Green's symmetric function modified in this way into (16) gives us accelerations from PHANTOM (8). Furthermore, substituting it into (17), we will conclude that the Newton's third law is fulfilled for any pair of cells, where the acceleration of particles is described by the formula (8).

4. Asymmetric interaction of kd-tree cells

In the previous section, we saw that the total force of interaction for any pair of cells is zero. This implies that if only the pairs of mutually interacting cells will appear in the calculation for estimating of the self-gravity forces for each particle at each computational time step, then all forces in the whole system will be

compensated with machine accuracy. At least with the accuracy of the errors resulting from the summation of a large amount of floating-points numbers [28–30].

In PHANTOM, at each calculation step after updating the kd-tree a paired well-separated remote cell is sought each leaf cell. It is important that such a pair is searched for only for leaf cells, but not for super-cells. As a result, in this method the direct pairs “leaf cell \leftarrow super-cell” will be encountered, but the reverse pairs will never be considered, which leads to asymmetry. The tree opening criterion (4) is also asymmetric in PHANTOM because it contains parameters of one cell only. An example of symmetric criteria is considered in [9; 31].

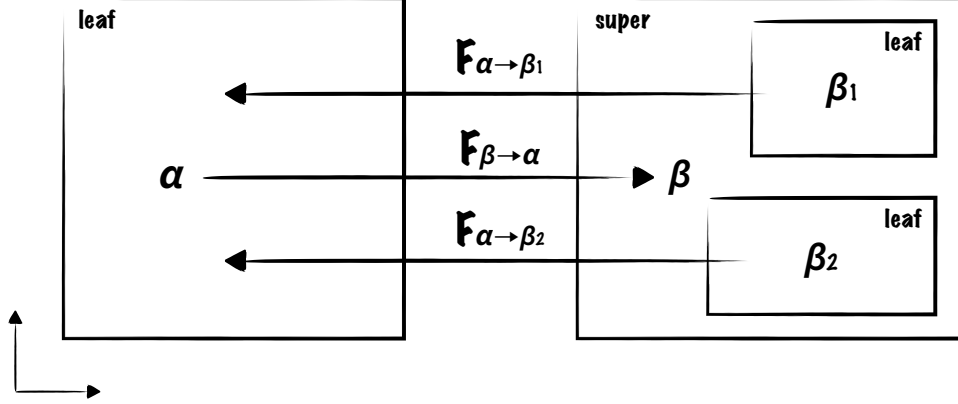


Figure 2. Non-symmetric gravitational interaction between SPH-particles of the leaf cell α and SPH-particles of the supercell β of the kd-tree. Details in the text.

A model of such a situation is illustrated in Fig. 2. A leaf cell α with mass M_α is attracted by the super-cell β with mass M_β with a force $F_{\beta \rightarrow \alpha}$. Let the centers of masses of the cells α and β be at the distance r . The super-cell consists of two leaf cells β_1 and β_2 , which attract α with the forces $F_{\alpha \rightarrow \beta_1}$ and $F_{\alpha \rightarrow \beta_2}$ respectively. The masses of these cells M_{β_1} and M_{β_2} add up to M_β . Let’s assume that $M_{\beta_2} > M_{\beta_1}$. Let the radius vector of the center of mass of the cell β_1 originating from the center of mass of the cell β be \mathbf{x} . Then the radius vector of the center of mass of the cell β_2 originating from the center of mass of the cell β is $-\mathbf{x}M_{\beta_1}/M_{\beta_2}$, by the definition of the center of mass β .

The i -component of the total force acting on the center of mass of the whole system is

$$F_i = F_{\beta \rightarrow \alpha, i} + F_{\alpha \rightarrow \beta_1, i} + F_{\alpha \rightarrow \beta_2, i} = \sum_{\mathbf{x} \in \alpha} m_p a_{\beta \rightarrow \alpha, i} + \sum_{\mathbf{x} \in \beta_1} m_p a_{\alpha \rightarrow \beta_1, i} + \sum_{\mathbf{x} \in \beta_2} m_p a_{\alpha \rightarrow \beta_2, i}, \quad (30)$$

where the expressions for accelerations are taken from (8) or, equivalently, from (28). The summation is carried out over the internal particles of each cell. All cell mass centers lie in the same plane P (Fig. 2 plane). Without limiting generality, let us arrange the coordinate system so that one axis passes through the centers of masses of the cells α and β , the second axis lies in the plane P , and the third axis is perpendicular to P .

Expanding F_i in a Taylor series by small displacement \mathbf{x} up to third order and writing out the leading terms, we get

$$F_1 \approx \frac{2}{r^5} M_\alpha M_\beta \frac{M_{\beta_1}}{M_{\beta_2}} \left(1 - \frac{M_{\beta_1}}{M_{\beta_2}}\right) (2x_1^2 - 3x_2^2)x_1, \quad (31)$$

$$F_2 \approx \frac{3}{2r^5} M_\alpha M_\beta \frac{M_{\beta_1}}{M_{\beta_2}} \left(1 - \frac{M_{\beta_1}}{M_{\beta_2}}\right) (x_2^2 - 4x_1^2)x_2.$$

The force component F_3 is zero with this accuracy. It is important to note that the expressions (31) do not involve the quadrupole moments of the cells, which means that the location of SPH-particles within each cell does not affect the force.

Maximizing the norm F of the vector \mathbf{F} for different \mathbf{x} , we obtain its following upper bound

$$F \approx \frac{4}{r^5} l^3 M_\alpha M_\beta \frac{M_{\beta_1}}{M_{\beta_2}} \left(1 - \frac{M_{\beta_1}}{M_{\beta_2}} \right), \quad (32)$$

where $l = |\mathbf{x}|$ is the distance from the center of mass of the cell β to the center of mass of the most distant cell. The resulting non-physical uncompensated force acts on each of the SPH-particles of the pair α, β . We will call such a pair of cells asymmetric.

Let us repeat this reasoning for the case if there are more than two leaf cells inside a supercell β , and instead of a leaf cell α , there can be a supercell with child leaf cells $\alpha_1, \alpha_2, \dots$. Assuming that cells with indices α_1, β_1 have the smallest masses, we get a generalization of the expression (32)

$$F \approx 4 \sum_{\alpha, \beta} \frac{M_\alpha M_\beta}{r_{\alpha\beta}^5} \left[\frac{M_{\alpha_1} l_{\alpha_1}^3}{M_\alpha - M_{\alpha_1}} \left(1 - \frac{M_{\alpha_1}}{M_\alpha - M_{\alpha_1}} \right) + \frac{M_{\beta_1} l_{\beta_1}^3}{M_\beta - M_{\beta_1}} \left(1 - \frac{M_{\beta_1}}{M_\beta - M_{\beta_1}} \right) \right]. \quad (33)$$

Here l_{α_1} and l_{β_1} are the distances from the centers of mass of α and β to the centers of mass of the lightest distant cells, respectively. Summation is performed over all possible asymmetric pairs α, β , the distances between which are $r_{\alpha\beta}$. If a cell α in some summand is a leaf cell, the first summand in square brackets in (33) is assumed to be zero, indicating that its size is also zero. It was not implied here that all cells necessarily lie in the same plane.

At some computational step there can be both asymmetric and symmetric pairs of cells. At the next step of the computation, when the kd-tree is updated, the number of pairs may change. For example, there may be a new asymmetric pair of cells oriented differently in space, or several pairs. The center of mass of the whole system (the whole kd-tree) experiences a “kick” F at each step in different directions. It can be said that an uncompensated random force will act on the system as a whole, causing it to shift from its initial position. The system ceases to be conservative, and we lose one of the main advantages of the SPH approach compared to the mesh method.

It is important to note that if in (30) instead of (8) we used the accelerations from (25) at $p = 3$, the resulting force would also be non-zero. Discarding terms with $1/r^5$ and above in the formula (30) does not solve the problem of the additional non-physical force. In the next section we will consider how the center of mass of the system will migrate due to its action.

5. Displacement of the system’s center of mass

Now let’s see how far the system as a whole shifts when it periodically receives a “kick” by a force described by an isotropic random variable f_i , whose modulus is uniformly distributed from zero to F . The time-average impact of such a force is $\langle f_i \rangle = 0$, and the RMS impact is $\langle f_i^2 \rangle = F^2/3$. Assume that the calculated time steps are equal for simplicity. Then, for each Δt , the system receives a momentum $f_i \Delta t$, or, similarly, it receives an additional velocity $\Delta v_i = f_i \Delta t / M$, where M is the mass of the system and

$$\langle \Delta v_i^2 \rangle = \frac{F^2}{3M} \Delta t^2. \quad (34)$$

We will consider one velocity component, e.g. x -component. The magnitudes of the velocity “kicks” at successive times are $\Delta v_1, \Delta v_2$, and so on. The velocity on the interval from k to $k + 1$ is

$$v_{k,k+1} = \sum_{i=1}^k \Delta v_i,$$

and the displacement is $S_{k,k+1} = v_{k,k+1} \Delta t$. The displacement on the interval from one to $k + 1$ is

$$S_{1,k+1} = \sum_{i=1}^k S_{i,i+1} = \Delta t \sum_{i=1}^k \Delta v_i (k - i + 1).$$

The average displacement $\langle S_i \rangle$ is zero because $\langle \Delta v_i \rangle = 0$, but the average square of the displacement is not zero

$$\langle S_{1,k+1}^2 \rangle = \Delta t^2 \sum_{i=1}^k \langle \Delta v_i^2 \rangle (k-i+1)^2,$$

where we take into account that $\langle \Delta v_i \Delta v_j \rangle = 0$ at $i \neq j$. The value $\langle \Delta v_i^2 \rangle$ can be considered independent on i . Then

$$\langle S_{1,k+1}^2 \rangle = \Delta t^2 \langle \Delta v_i^2 \rangle \sum_{i=1}^k i^2.$$

The sum here is $k(k+1)(2k+1)/6 \simeq k^3/3$ for $k \gg 1$ and $k = T/\Delta t$, where T is the observation time of the system. Finally, for the total displacement

$$\langle r^2 \rangle = \langle S_x^2 \rangle + \langle S_y^2 \rangle + \langle S_z^2 \rangle,$$

we obtain

$$\sqrt{\langle r^2 \rangle} = \frac{F}{M} \sqrt{\frac{\Delta t}{3}} T^{\frac{3}{2}}. \quad (35)$$

The amount of momentum transferred is random. This means that the velocities are the sum of many “jumps” in momentum space. We can state that the action of a chaotic force on a system leads to random walks in momentum space. Hence

$$\langle v_{k,k+1}^2 \rangle = k \langle \Delta v_i^2 \rangle,$$

where $\langle v_{k,k+1}^2 \rangle$ is the average square of the speed that the system has in the interval from k to $k+1$. If we rewrite the latter expression as a function of time and take into account (34), we get

$$\sqrt{\langle v^2 \rangle} = \frac{F}{M} \sqrt{\frac{\Delta t}{3}} T^{\frac{1}{2}}. \quad (36)$$

This shows that the velocity increases infinitely with time. Using (36) we can also define the standard deviation of the random variable of the linear momentum of the system

$$\sqrt{\langle p^2 \rangle} = M \sqrt{\langle v^2 \rangle}. \quad (37)$$

A non-diffusive random walk law $|r(T)| \propto T^{3/2}$ follows from equation (35) (in the case of diffusion it would be $|r(T)| \propto T^{1/2}$). This deviation arises because the system “remembers” the prehistory of its motion, accumulating momentum while violating the condition of independence of successive steps. The displacement of the system’s center of mass due to a small chaotic change in its velocity for each counting step is called a random memory walk [32].

Now that we know what the force of the “kick” depends on, let’s find out what affects its frequency. In PHANTOM, at the end of each numerical step, the Δt of the next step is determined as the minimum of all kinds of time step constraints on all SPH-particles. Usually, the strictest constraint during the calculation follows from the Courant–Friedrichs–Lewy condition [17]. Using this condition, we obtain

$$\Delta t = C_{\text{cour}} \min_p \frac{h_p}{\max_n v_{\text{sig,pn}}}, \quad (38)$$

where $C_{\text{cour}} = 0.3$ by default [33],

$$h_p = h_{\text{fact}} \left(\frac{m_p}{\rho_p} \right)^{\frac{1}{3}} \quad (39)$$

is the smoothing length, h_{fact} is a numerical parameter close to unity and

$$v_{\text{sig,pn}} = \alpha_p^{\text{AV}} c_{\text{s,p}} + \beta^{\text{AV}} |v_p \cdot \hat{r}_{\text{pn}}| \quad (40)$$

is the maximum signal speed, which is a multiplier in the artificial viscosity tensor [17]. Here $\alpha_p^{\text{AV}}, \beta^{\text{AV}}$ are dimensionless constants of order of unity, the exact values of which are not important now,

$$v_{\text{pn}} \equiv v_p - v_n, \quad \hat{r}_{\text{pn}} \equiv (r_p - r_n) / |r_p - r_n|,$$

and the speed of sound is

$$c_{s,p} = \sqrt{\frac{\gamma P_p}{\rho_p}}, \quad (41)$$

where P_p is pressure, and ρ_p is a density. The artificial viscosity for the SPH method contains both a linear velocity term at the multiplier α_p^{AV} , analogous to shear and bulk viscosity, and a second-order Von Neumann-Richtmyer-like term [34] that prevents particle interpenetration. Let us restrict ourselves to the case of the polytropic equation of state of matter

$$P_p = K \rho_p^\gamma. \quad (42)$$

Combining (39)–(42) and substituting into (38) for the case of hydrostatic equilibrium (when $v_{\text{pn}} = 0$), we obtain

$$\Delta t \propto m_p^{\frac{1}{3}} \rho^{\frac{(1-\gamma)}{2} - \frac{1}{3}}. \quad (43)$$

In the next section we will explicitly demonstrate the displacement of the system’s center of mass in the PHANTOM calculations.

6. Non-conservation of the total linear momentum of the system in PHANTOM

To illustrate the non-conservation of the total momentum, we will consider the model of a single NS. To do this, in PHANTOM we will “assemble” a ball out of N SPH-particles with radius $R = 10$ km and mass $M = 1M_\odot$, with a density profile satisfying the equation of state polytropes with $n = 1$ (adiabatic index of the matter $\gamma = 2$). This simple polytrope well describes the equation of state of NS in the intermediate mass range $1M_\odot \leq M \leq 2M_\odot$ [35]. All SPH-particle masses assumed to be the same and equal to

$$m_p \equiv M/N. \quad (44)$$

The particles are initially arranged uniformly and isotropically in space and then distributed in accordance with the requirements of the given density profile and radius with preservation of the relative arrangement along the mass coordinate (stretch mapping, [17]). The initial velocities of all particles are zero. The constructed star is already close to equilibrium. The diameter of a star in equilibrium is of the order of the critical Jeans wavelength. This means that it is impossible to place disturbances inside the star that would increase and it is always stable with respect to fragmentation into many small parts [36]. The goal is to bring the NS to a state of complete equilibrium. This process is called relaxation in PHANTOM.

The relaxation simulation starts from the aforesaid initial model and the complete system of dynamic equations of motion of self-gravitating particles is solved in the SPH approximation. This system is described by equations (23) and (24) and their SPH approximation is given by equations (34) and (35) in [17].

In the following calculations the cubic spline kernel M_4 is used [eq. 17 in 17; 37] and the compact support of the function implies that $R_{\text{kern}} = 2$. The choice of $h_{\text{fact}} = 1.2$ for the M_4 cubic spline kernel is based on the fact that it is slightly less than the maximum neighbour number that can be used while remaining stable to the pairing instability [16; 17; 38]. The mean neighbour number can be estimated as $\bar{N}_{\text{neigh}} = \frac{4}{3}\pi (R_{\text{kern}} h_{\text{fact}})^3$, which for M_4 kernel corresponds to 57.9 neighbours for particles with a uniform density distribution. The actual number of neighbours of SPH-particle occurring in calculations for the case of NS with $N = 5000$ is $\sim 65_{-13}^{+15}$ and with $N = 150000$ is $\sim 63_{-11}^{+10}$. As one can see, these values are in good agreement with the estimate \bar{N}_{neigh} .

The average smoothing length is $h_p \approx 0.97$ km for $N = 5000$. It follows from equations (39) and (44) that h_p decreases with increasing N as $N^{-1/3}$. Therefore, for the full range of N considered below, the values of h_p are significantly smaller than R , which results in the existence of pairs of well-separated cells.

The calculation results for the cases with different numbers of SPH-particles are presented below. The distance unit is $u_{\text{dist}} = 1$ km, the mass unit is $u_{\text{mass}} = 1M_\odot$, the time unit in accordance with (1) is $u_{\text{time}} = 2.75 \cdot 10^{-6}$ s, and the tree opening parameter θ from (4) is 0.5. We take the duration of the simulation from the following considerations: a close binary system of identical NSs with the above parameters makes dozens of orbital revolutions in a time $\sim 4 \cdot 10^4 [u_{\text{time}}]$.

The flattening $(a - b)/a$ is demonstrated at Fig. 3, where a and b are the semi-axes of the star’s ellipsoid. Here, the NS quickly reaches an equilibrium state at $t \approx 5000 [u_{\text{time}}]$ and until the end of the simulation the star moves as a whole slightly pulsating.

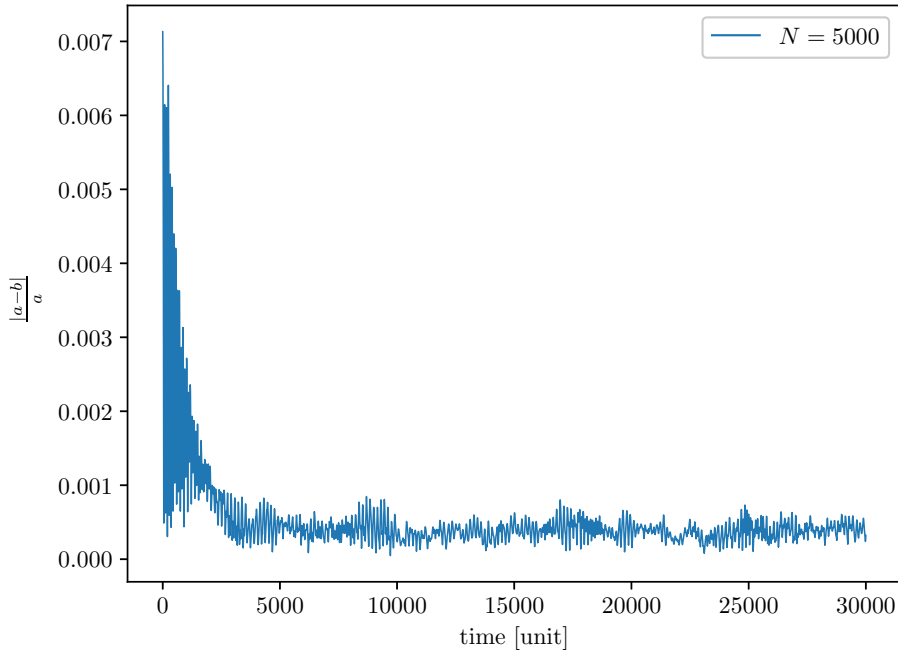


Figure 3. Flattening of the neutron star ellipsoid, calculated at SPH-particle number $N = 5000$ and $\theta = 0.5$.

The behavior of the random variables over time is presented at Fig. 4 and 5: r_{com}/R is the deviation of the center of mass of the NS from the initial position, normalized to its radius, and p is the linear momentum of the NS for six different numbers of SPH-particles at $\theta = 0.5$. The standard deviation of the random variable r_{com} is defined in (35), and the standard deviation of the momentum is taken from (37). It can be seen (Fig. 4) that the NS is shifted from its initial position by a distance comparable to its size! Neither the linear momentum of the system (Fig. 5) nor the angular momentum are conserved (Fig. 6). The latter means that the matter inside the NS has a non-zero angular velocity. However, the study of this observation is beyond the scope of the present article.

If we perform the same calculation with the parameter $\theta = 0$ for the tree opening criterion (4), when all gravitational forces in the system are calculated by direct summation, then there will be no such a displacement of the center of mass of the system (see Fig. 7). This proves that the main influence on the effect of non-conservativity is exerted by the gravitational forces of long-range interaction and the displacement is not connected with SPH properties of the system.

Let us estimate which parameters affect the magnitude of the total linear momentum of the star using the results of the section 4. For estimation, we assume that all leaf cells have the same mass

$$M_l = 10 m_p. \quad (45)$$

Although in practice there are cells in which the number of SPH-particles is less than 10, the vast majority contains just the maximum allowable number of particles when constructing a kd-tree. Then, let's introduce the numbers of leaf cells in super-cells α and β are $N_\alpha = M_\alpha/M_l$ and $N_\beta = M_\beta/M_l$ respectively. Finally, remembering that $l_{\alpha_1}, l_{\beta_1}$ are the distances to the most distant leaf cells, we will assume that they are also the characteristic sizes s_{α_1} and s_{β_1} of their parent cells, respectively. If α is a leaf cell in some term, then we will assume that its size is zero. Then (33) will have the following form

$$F \approx 4M_l^2 \sum_{\alpha, \beta} \frac{N_\alpha N_\beta}{r_{\alpha\beta}^5} \left[s_\alpha^3 \frac{(N_\alpha - 2)}{(N_\alpha - 1)^2} + s_\beta^3 \frac{(N_\beta - 2)}{(N_\beta - 1)^2} \right]. \quad (46)$$

When the total number of particles N changes in any super-cell, the number of its leaf cells will change as a piecewise-constant function taking values close to the function proportional to $N/10$. This means that N_α and N_β are close to the linear function of N . Further, since every pair of cells in the sum (46) by construction

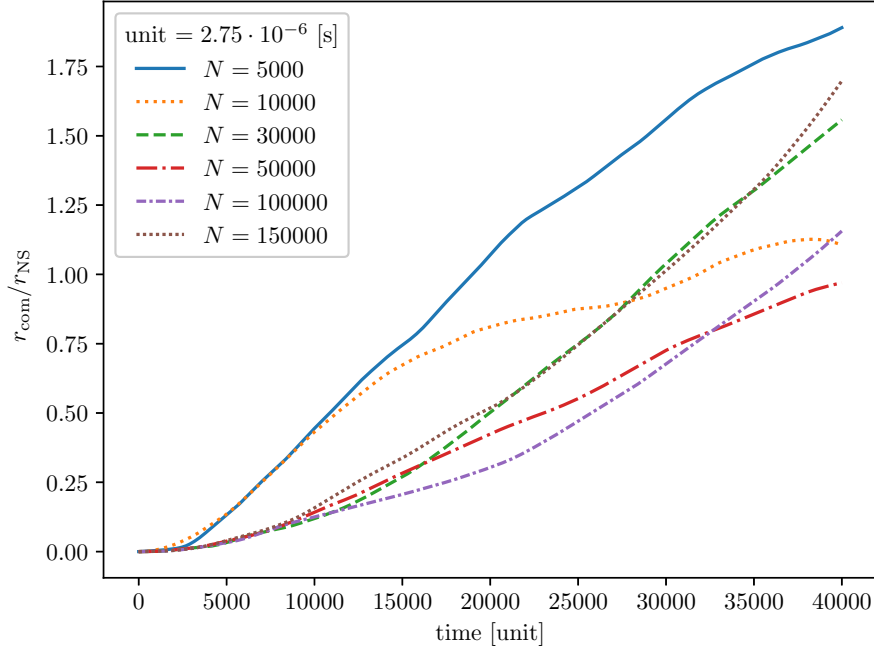


Figure 4. The displacement of the center of mass of a single neutron star normalized by its radius, calculated for six different numbers of SPH-particles at $\theta = 0.5$.

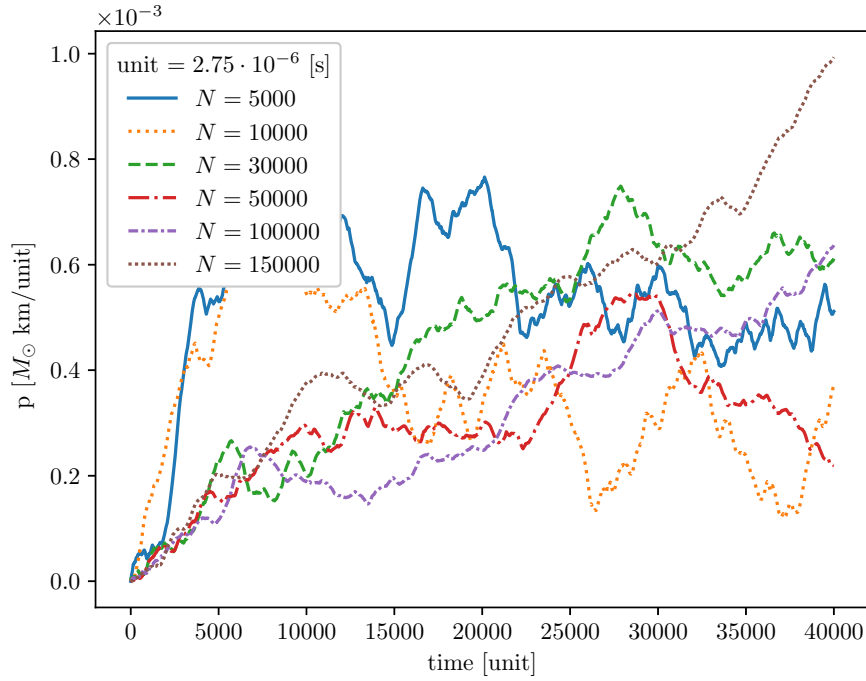


Figure 5. The linear momentum of a single neutron star, calculated for six different numbers of SPH-particles at $\theta = 0.5$.

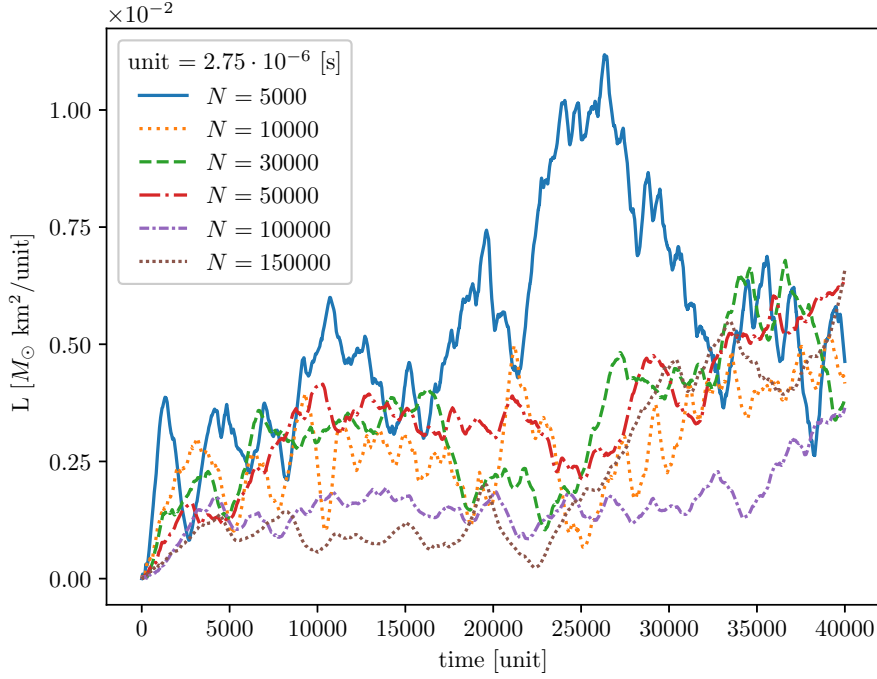


Figure 6. The angular momentum of a single neutron star, calculated for six different numbers of SPH-particles at $\theta = 0.5$.

does not satisfy the tree opening criterion (4), then $(s_\alpha/r_{\alpha\beta})^3$ and $(s_\beta/r_{\alpha\beta})^3$ are majorized by the parameter $\theta^{3/2}$. It follows from (44) and (45) that $M_l \propto M/N$, and any distance between cells $r_{\alpha\beta} \propto R$. The number of pairs of asymmetric cells in the sum (46) varies proportionally to the function $N^{\sigma+1}$, where $0 \leq \sigma \leq 1$, and depends on the value of the parameter θ , which determines the number of interaction participants. Summarizing the foregoing, we get that

$$F \propto (M/R)^2 N^\sigma. \quad (47)$$

Assuming that the average density of NS is

$$\rho = M \left(\frac{4}{3} \pi R^3 \right)^{-1}, \quad (48)$$

it is possible to obtain from (44) and (43) that

$$\Delta t \propto M^{\frac{(1-\gamma)}{2}} R^{1-\frac{3(1-\gamma)}{2}} N^{-\frac{1}{3}}. \quad (49)$$

Finally, substituting (47) and (49) into (35), we get

$$\sqrt{\langle r^2 \rangle} \propto M^{\frac{(5-\gamma)}{4}} R^{\frac{3(\gamma-3)}{4}} N^{\sigma-\frac{1}{6}} T^{\frac{3}{2}}. \quad (50)$$

The obtained formula (50) is also true for any ball of SPH-particles. Let us write out three special cases: for NS intermediate mass ($\gamma = 2$)

$$\sqrt{\langle r^2 \rangle} \propto \left(\frac{M}{R} \right)^{\frac{3}{4}} N^{\sigma-\frac{1}{6}} T^{\frac{3}{2}}, \quad (51)$$

for a white dwarf (WD) ($\gamma = 5/3$)

$$\sqrt{\langle r^2 \rangle} \propto \frac{M^{\frac{5}{6}}}{R} N^{\sigma-\frac{1}{6}} T^{\frac{3}{2}}, \quad (52)$$

and for relativistic matter (Chandrasekhar WD or a large hot star) ($\gamma = 4/3$)

$$\sqrt{\langle r^2 \rangle} \propto M^{\frac{11}{12}} R^{-\frac{5}{4}} N^{\sigma-\frac{1}{6}} T^{\frac{3}{2}}. \quad (53)$$

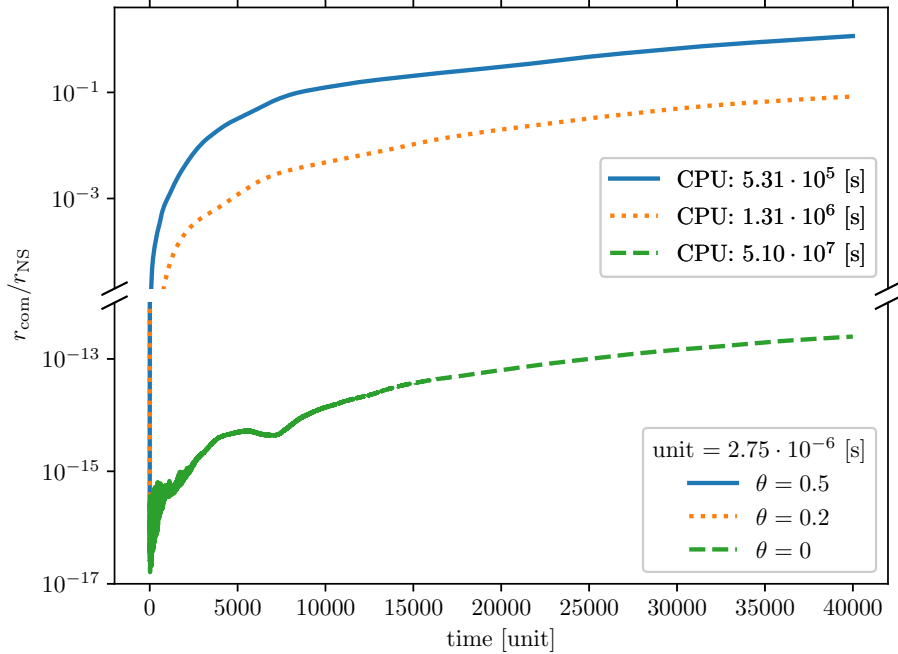


Figure 7. The displacement of the center of mass of a single neutron star normalized by its radius, calculated for three different values of θ with the number of particles $N = 100000$. CPU time consumption on AMD Ryzen 7 2700X Eight-Core Processor machine are presented for all three cases of value θ .

It is clear from (52) that if our ball from the example above with $\theta = 0.5$ is “stretched” by a factor of 600 to the size of the WD, leaving the mass of $1M_{\odot}$, the displacement error will also decrease by a factor of ~ 600 and will be only $\sim 0.0003\%$ of the radius of the WD ~ 6000 km at $\sim 4 \cdot 10^4 [u_{\text{time}}]$. This means that the PHANTOM code can be used without corrections for objects like WD, not to mention large stars (53) or planetary nebulae. It should be noted, however, that if we consider much larger timescales, covering dozens of orbital revolutions, for example in the case of a WD binary system – the resulting error in the center of mass displacement also becomes comparable to the radius of a WD.

However, from (51) it follows that for $\sigma > 1/6$, no changes in N can eliminate the error in the displacement of the center of mass for NS. To estimate σ we construct the fit N^{σ} of the function $F(N) = \max_i f_i(T, N)$.

For random variables of modulus of the uncompensated force $f_i(T, N)$ with $\theta = 0.5$ (see Fig. 8) the value of σ is about 0.55. The same fitting for different values of tree opening parameter θ shows that σ is a monotonically increasing function of θ . At $\theta = 0.2$ this function takes the value $\sigma \approx 0.15$, which is slightly less than $1/6 \approx 0.16$.

Thus, for values of the tree opening parameter $\theta \gtrsim 0.2$, the standard deviation $\sqrt{\langle r^2 \rangle}$ will grow with increasing N , while for small $\theta \lesssim 0.2$ it will decrease. One can always find such a pair N and $0 < \theta < 0.2$, where the error for NS becomes negligible.

However, we can see from the formula (51) that for any small θ the lower bound on the standard deviation $\sqrt{\langle r^2 \rangle}$ is a very slow function $N^{-1/6}$. Thus, to reduce the error by one order the number of SPH-particles should be increased by 6 orders of magnitude. In its turn, for any fixed N , the decrease of θ leads to an increase of the radius $r \sim 1/\theta$ of the short-range interaction region and to the dominance of a_{short} defined in (3). This leads to a significant rise in computation time (see Fig. 7). This means that in order to use PHANTOM in calculations for objects like NS, it is necessary to correct the system for non-conservativity problems we demonstrated above.

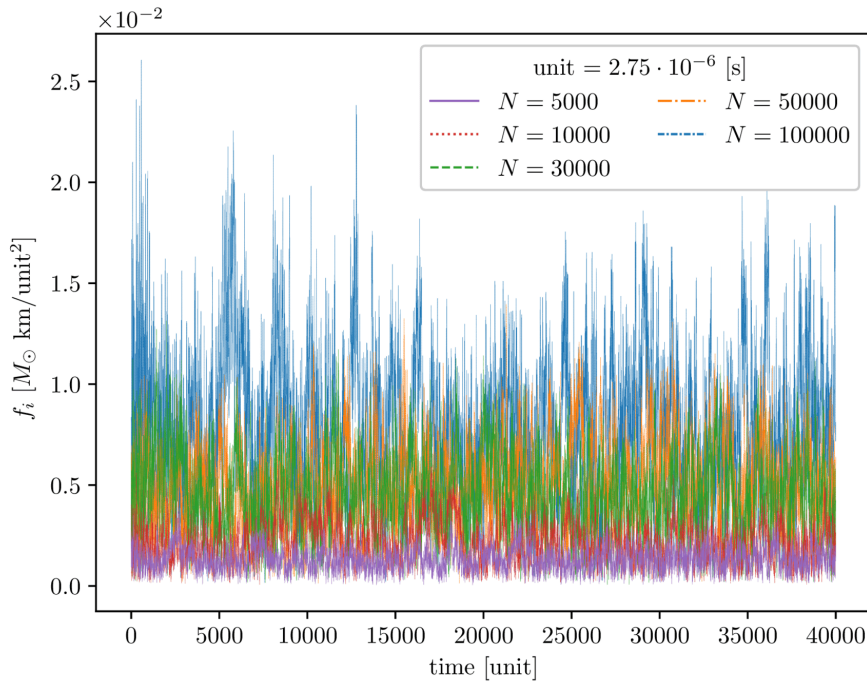


Figure 8. The modulus of the uncompensated force acting on the center of mass of a single neutron star calculated for three different numbers of SPH-particles at $\theta = 0.5$.

7. Conclusion

In this article, we discussed a way to implement the FMM in the PHANTOM code for calculation of the self-gravity forces. The code is widely used in various fields of astrophysics [18–23].

The standard implementation of the FMM (see, e.g., [9; 10]) implies the second order Taylor expansion of the gravitational interaction force between two cells of the kd-tree by small displacements of the source-particle and the sink-particle expressed through the vector \mathbf{r} connecting the centers of these cells. Thus, the maximum degree of $1/r$ will be 4. In contrast, in PHANTOM, such expansion is carried out step-by-step. The initial step is to perform the second order Taylor expansion for the small displacements of the source-particle. Afterwards, the second order Taylor expansion is carried out for the small displacements of the sink-particle. The maximum degree of $1/r$ in this case will be 6. In this paper, it was shown that even with this method of recording the force for any pair of kd-tree cells, in the case of mutual interaction the Newton’s third law is satisfied. However, linear momentum is not conserved for the entire system. This fact is explained by that only pairs of kd-tree cells “leaf cell \leftarrow super-cell” are considered in PHANTOM. Reverse pairs are not considered. In contrast, the method outlined in [9; 10] involves recursive tree-walk, whereby all possible symmetric pairs of well-separated cells of all types are considered, in accordance with the symmetric opening criterion.

It was shown in the paper that an additional non-physical force, resulting from the non-conservation of linear momentum, causes the system as a whole to migrate. The law of this migration is described by random memory walk. Using the example of a system describing a NS, it was demonstrated how the magnitude of the mean-square displacement of the center of mass of the star from its initial position depends on the mass of the star, its radius, and the number of SPH-particles in it. In the case of using PHANTOM for hydrodynamic modelling of objects with NS characteristics, the shift can indeed be significant. Thus, for a pair of NS, the displacement of the center of mass is comparable to the radius of NS at the time of a few tens Keplerian revolutions of the pair. For nebulae, hot stars and even WD such a shift can be considered to be negligibly small over the same duration.

It was explained that increasing the number of SPH-particles does not lead to a decrease of this displacement at values of the tree opening parameter $\theta \gtrsim 0.2$. The displacement error reduces as the tree opening parameter $\theta \lesssim 0.2$ become smaller, but this leads to a significant growth in computation time. This means that the

PHANTOM requires a correction using the method [9; 10]. However, it is well known that the FMM method, even in its realisation [9; 10], is inherent in the non-conservation of the angular momentum of the system [39]. This aspect requires further investigation. For conservativity in both linear and angular momentum the current implementation of PHANTOM requires corrections.

The authors would like to thank S.I. Blinnikov for useful discussions and important comments and to O.G. Olkhovskaya for assistance in translation. The authors are grateful to the anonymous referee for valuable comments.

References

1. Barnes J., Hut P. A Hierarchical $O(N \log N)$ Force-Calculation Algorithm // *Nature*. — 1986. — Dec. — Vol. 324, no. 6096. — P. 446–449. — DOI: [10.1038/324446a0](https://doi.org/10.1038/324446a0). — (Cit. on p. 1).
2. Greengard L., Rokhlin V. A Fast Algorithm for Particle Simulations // *Journal of Computational Physics*. — 1997. — Aug. — Vol. 135, no. 2. — P. 280–292. — DOI: [10.1006/jcph.1997.5706](https://doi.org/10.1006/jcph.1997.5706). — (Cit. on pp. 1, 3).
3. Capuzzo-Dolcetta R., Miocchi P. A Comparison between the Fast Multipole Algorithm and the Tree-Code to Evaluate Gravitational Forces in 3-D // *Journal of Computational Physics*. — 1998. — June. — Vol. 143, no. 1. — P. 29–48. — DOI: [10.1006/jcph.1998.5949](https://doi.org/10.1006/jcph.1998.5949). — arXiv: [astro-ph/9703122](https://arxiv.org/abs/astro-ph/9703122). — (Cit. on p. 1).
4. Gumerov N. A., Duraiswami R. *Fast Multipole Methods for the Helmholtz Equation in Three Dimensions*. — Amsterdam London : Elsevier, 2004. — (Elsevier Series in Electromagnetism). — (Cit. on p. 1).
5. Gumerov N. Fast Multipole Method // *Vestn. Akad. Nauk Resp. Bashkortostan*. — 2013. — Vol. 18, no. 4. — P. 11–24. — (Cit. on p. 1).
6. Hockney R., Eastwood J. *Computer Simulation Using Particles*. — CRC Press, 2021. — (Cit. on p. 1).
7. Nitadori K. Particle Mesh Multipole Method: An Efficient Solver for Gravitational/Electrostatic Forces Based on Multipole Method and Fast Convolution over a Uniform Mesh. — 10/17/2014. — arXiv: [1409.5981](https://arxiv.org/abs/1409.5981) [[astro-ph](https://arxiv.org/abs/astro-ph), [physics:physics](https://arxiv.org/abs/physics/physics)]. — URL: <http://arxiv.org/abs/1409.5981> (visited on 06/11/2024). — preprint. — (Cit. on p. 1).
8. Wang Q. A Hybrid Fast Multipole Method for Cosmological N-body Simulations // *Research in Astronomy and Astrophysics*. — 2021. — Jan. 1. — Vol. 21, no. 1. — P. 003. — DOI: [10.1088/1674-4527/21/1/3](https://doi.org/10.1088/1674-4527/21/1/3). — (Cit. on p. 1).
9. Dehnen W. A Very Fast and Momentum-conserving Tree Code // *The Astrophysical Journal*. — 2000. — June 10. — Vol. 536, no. 1. — P. L39–L42. — DOI: [10.1086/312724](https://doi.org/10.1086/312724). — (Cit. on pp. 1, 2, 5–7, 15, 16).
10. Dehnen W. A Hierarchical (N) Force Calculation Algorithm // *Journal of Computational Physics*. — 2002. — June. — Vol. 179, no. 1. — P. 27–42. — DOI: [10.1006/jcph.2002.7026](https://doi.org/10.1006/jcph.2002.7026). — arXiv: [astro-ph/0202512](https://arxiv.org/abs/astro-ph/0202512). — (Cit. on pp. 1, 2, 6, 15, 16).
11. Gafton E., Rosswog S. A Fast Recursive Coordinate Bisection Tree for Neighbour Search and Gravity // *Mon. Notices Royal Astron. Soc.* — 2011. — Sept. 15. — Vol. 418, no. 2. — P. 770–781. — DOI: [10.1111/j.1365-2966.2011.19528.x](https://doi.org/10.1111/j.1365-2966.2011.19528.x). — (Cit. on pp. 1, 2).
12. Dehnen W. A Fast Multipole Method for Stellar Dynamics // *Comput. Astrophys.* — 2014. — Sept. — Vol. 1, no. 1. — P. 1. — DOI: [10.1186/s40668-014-0001-7](https://doi.org/10.1186/s40668-014-0001-7). — (Cit. on pp. 1, 3, 5).
13. Marcello D. C., Shiber S., De Marco O., [et al.]. octo-Tiger: A New, 3D Hydrodynamic Code for Stellar Mergers That Uses hpx Parallelization // *Mon. Notices Royal Astron. Soc.* — 2021. — Apr. 10. — Vol. 504, no. 4. — P. 5345–5382. — DOI: [10.1093/mnras/stab937](https://doi.org/10.1093/mnras/stab937). — arXiv: [2101.08226](https://arxiv.org/abs/2101.08226). — (Cit. on p. 1).
14. Bentley J. L. Multidimensional Binary Search Trees Used for Associative Searching // *Communications of the ACM*. — 1975. — Sept. — Vol. 18, no. 9. — P. 509–517. — DOI: [10.1145/361002.361007](https://doi.org/10.1145/361002.361007). — (Cit. on p. 1).
15. Potter D., Stadel J., Teyssier R. PKDGRAV3: Beyond Trillion Particle Cosmological Simulations for the next Era of Galaxy Surveys // *Computational Astrophysics and Cosmology*. — 2017. — May 18. — Vol. 4, no. 1. — P. 2. — DOI: [10.1186/s40668-017-0021-1](https://doi.org/10.1186/s40668-017-0021-1). — (Cit. on p. 1).
16. Price D. J. Smoothed particle hydrodynamics and magnetohydrodynamics // *Journal of Computational Physics*. — 2012. — Feb. — Vol. 231, no. 3. — P. 759–794. — DOI: [10.1016/j.jcp.2010.12.011](https://doi.org/10.1016/j.jcp.2010.12.011). — arXiv: [1012.1885](https://arxiv.org/abs/1012.1885). — (Cit. on pp. 1, 2, 10).

17. Price D. J., Wurster J., Tricco T. S., [et al.]. Phantom : A Smoothed Particle Hydrodynamics and Magnetohydrodynamics Code for Astrophysics // Publications of the Astronomical Society of Australia. — 2018. — Sept. — Vol. 35, no. 2018. — e031. — DOI: [10.1017/pasa.2018.25](https://doi.org/10.1017/pasa.2018.25). — arXiv: [1702.03930](https://arxiv.org/abs/1702.03930). — (Cit. on pp. 1, 3, 5, 9, 10).
18. Pinte C., Price D. J., Ménard F., [et al.]. Kinematic Evidence for an Embedded Protoplanet in a Circumstellar Disk // The Astrophysical Journal Letters. — 2018. — June. — Vol. 860, no. 1. — P. L13. — DOI: [10.3847/2041-8213/aac6dc](https://doi.org/10.3847/2041-8213/aac6dc). — arXiv: [1805.10293](https://arxiv.org/abs/1805.10293) [[astro-ph.SR](#)]. — (Cit. on pp. 2, 15).
19. Golightly E. C. A., Coughlin E. R., Nixon C. J. Tidal Disruption Events: The Role of Stellar Spin // The Astrophysical Journal. — 2019. — Feb. — Vol. 872, no. 2. — P. 163. — DOI: [10.3847/1538-4357/aafd2f](https://doi.org/10.3847/1538-4357/aafd2f). — arXiv: [1901.03717](https://arxiv.org/abs/1901.03717) [[astro-ph.HE](#)]. — (Cit. on pp. 2, 15).
20. Heath R. M., Nixon C. J. On the orbital evolution of binaries with circumbinary discs // Astronomy and Astrophysics. — 2020. — Sept. — Vol. 641. — A64. — DOI: [10.1051/0004-6361/202038548](https://doi.org/10.1051/0004-6361/202038548). — arXiv: [2007.11592](https://arxiv.org/abs/2007.11592) [[astro-ph.HE](#)]. — (Cit. on pp. 2, 15).
21. Blinnikov S. I., Yudin A. V., Kramarev N., Potashov M. Stripping Model for Short Gamma-Ray Bursts in Neutron Star Mergers // Particles. — 2022. — June 16. — Vol. 5, no. 2. — P. 198–209. — DOI: [10.3390/particles5020018](https://doi.org/10.3390/particles5020018). — (Cit. on pp. 2, 15).
22. Potashov M. S., Yudin A. V. Algorithm for Taking into Account Back-Reaction of Gravitational Waves Emission during the Merger of Neutron Stars // Keldysh Institute Preprints. — 2023. — Vol. 2898, no. 40. — P. 1–17. — DOI: [10.20948/prepr-2023-40](https://doi.org/10.20948/prepr-2023-40). — (Cit. on pp. 2, 15).
23. Yudin A., Blinnikov S., Kramarev N., Potashov M. Merging and striping regimes in close pairs of relativistic stars: prospects for models of short gamma-bursts // Izvestiya VUSov (Radiophysics). — 2023. — Apr. 18. — Vol. 66, no. 9. — P. 720–734. — DOI: [10.52452/00213462_2023_66_09_720](https://doi.org/10.52452/00213462_2023_66_09_720). — (Cit. on pp. 2, 15).
24. Potashov M. S. Non-Conservation of Momentum in the FMM Method in the PHANTOM Code // Keldysh Institute Preprints. — 2024. — No. 43. — P. 1–25. — DOI: [10.20948/prepr-2024-43](https://doi.org/10.20948/prepr-2024-43). — (Cit. on p. 2).
25. Price D. J., Monaghan J. J. An Energy-Conserving Formalism for Adaptive Gravitational Force Softening in Smoothed Particle Hydrodynamics and N-body Codes // Mon. Notices Royal Astron. Soc. — 2007. — Feb. — Vol. 374, no. 4. — P. 1347–1358. — DOI: [10.1111/j.1365-2966.2006.11241.x](https://doi.org/10.1111/j.1365-2966.2006.11241.x). — (Cit. on pp. 3–5).
26. Bogolyubov A., Levashova N., Mogilevskiy I., [et al.]. Green’s Function of the Laplace Operator. — 2018. — (Cit. on p. 4).
27. Folland G. B. Advanced Calculus. — Upper Saddle River, NJ : Prentice Hall, 2002. — 461 p. — (Cit. on p. 5).
28. Lange M., Rump S. M. Error Estimates for the Summation of Real Numbers with Application to Floating-Point Summation // BIT Numerical Mathematics. — 2017. — May 3. — Vol. 57, no. 3. — P. 927–941. — DOI: [10.1007/s10543-017-0658-9](https://doi.org/10.1007/s10543-017-0658-9). — (Cit. on p. 7).
29. Rhyne J. Probabilistic Error Analysis For Sequential Summation of Real Floating Point Numbers. — 05/28/2021. — arXiv: [2101.11738](https://arxiv.org/abs/2101.11738) [[cs](#), [math](#)]. — URL: <http://arxiv.org/abs/2101.11738> (visited on 05/05/2024). — preprint. — (Cit. on p. 7).
30. Hallman E., Ipsen I. C. F. Deterministic and Probabilistic Error Bounds for Floating Point Summation Algorithms. — 07/04/2021. — arXiv: [2107.01604](https://arxiv.org/abs/2107.01604) [[cs](#), [math](#)]. — URL: <http://arxiv.org/abs/2107.01604> (visited on 05/05/2024). — preprint. — (Cit. on p. 7).
31. Loiseau J., Lim H., Kaltenborn M. A., [et al.]. FleCSPH: The next Generation FleCSible Parallel Computational Infrastructure for Smoothed Particle Hydrodynamics // SoftwareX. — 2020. — July. — Vol. 12. — P. 100602. — DOI: [10.1016/j.softx.2020.100602](https://doi.org/10.1016/j.softx.2020.100602). — (Cit. on p. 7).
32. Popov P. Diffusion. — Moscow : Mipt, 2016. — (Cit. on p. 9).
33. Lattanzio J. C., Monaghan J. J., Pongracic H., Schwarz M. P. Controlling Penetration // SIAM Journal on Scientific and Statistical Computing. — 1986. — Apr. — Vol. 7, no. 2. — P. 591–598. — DOI: [10.1137/0907039](https://doi.org/10.1137/0907039). — (Cit. on p. 9).
34. VonNeumann J., Richtmyer R. D. A Method for the Numerical Calculation of Hydrodynamic Shocks // Journal of Applied Physics. — 1950. — Mar. 1. — Vol. 21, no. 3. — P. 232–237. — DOI: [10.1063/1.1699639](https://doi.org/10.1063/1.1699639). — (Cit. on p. 10).
35. Greif S. K., Hebel K., Lattimer J. M., [et al.]. Equation of State Constraints from Nuclear Physics, Neutron Star Masses, and Future Moment of Inertia Measurements // The Astrophysical Journal. — 2020. — Oct. 1. — Vol. 901, no. 2. — P. 155. — DOI: [10.3847/1538-4357/abaf55](https://doi.org/10.3847/1538-4357/abaf55). — (Cit. on p. 10).

36. Zeldovich Y. B., Novikov I. D. *Relativistic Astrophysics*. — Moscow : Nauka, 1967. — (Cit. on p. 10).
37. Schoenberg I. J. Contributions to the Problem of Approximation of Equidistant Data by Analytic Functions. Part A. On the Problem of Smoothing or Graduation. A First Class of Analytic Approximation Formulae // *Quarterly of Applied Mathematics*. — 1946. — Vol. 4, no. 1. — P. 45–99. — DOI: [10.1090/qam/15914](https://doi.org/10.1090/qam/15914). — (Cit. on p. 10).
38. Rosswog S. SPH Methods in the Modelling of Compact Objects // *Living Reviews in Computational Astrophysics*. — 2015. — Oct. 19. — Vol. 1, no. 1. — P. 1. — DOI: [10.1007/lrca-2015-1](https://doi.org/10.1007/lrca-2015-1). — (Cit. on p. 10).
39. Marcello D. C. A Very Fast and Angular Momentum Conserving Tree Code // *The Astronomical Journal*. — 2017. — Aug. — Vol. 154, no. 3. — P. 92. — DOI: [10.3847/1538-3881/aa7b2f](https://doi.org/10.3847/1538-3881/aa7b2f). — (Cit. on p. 16).